RSC Advances

PAPER

View Article Online
View Journal | View Issue

Cite this: *RSC Adv.*, 2026, **16**, 13749

Enhancing microbial electrosynthesis of fatty acids from carbon dioxide by combining bioaugmentation of an acetogenic enrichment and Fe–Sn oxide cathode coating

Tambakassi Mihin,[ab] Lars Schreiber,[b] Oumarou Savadogo[a] and Boris Tartakovsky *[b]

This study evaluated the impact of bioaugmenting a mixed acetogenic enrichment with *Clostridium kluyveri* on CO_2 reduction to fatty acids, specifically butyrate and caproate, in a microbial electrosynthesis (MES) cell equipped with an Fe-Sn oxide – coated cathode. Without bioaugmentation, at a volumetric CO_2 inflow of 1.67 L_{CO2} (L_c d)$^{-1}$ (per cathode chamber volume) approximately 86% of the CO_2 was converted to the target products, leading to maximum production rates of butyrate and caproate of 875 mg (L_c d)$^{-1}$ and 94 mg (L_c d)$^{-1}$, respectively. With inoculum bioaugmentation and ethanol supplementation, CO_2 conversion reached 85% at a higher inflow rate of 2.78 L_{CO2} (L_c d)$^{-1}$ and the production of butyrate and caproate reached 733 mg (L_c d)$^{-1}$ and 792 mg (L_c d)$^{-1}$, respectively. Biomolecular analysis of microbial populations confirmed the proliferation of the bioaugmented *C. kluyveri* in cathodic biofilms and liquid, however only under an external ethanol supply. In addition, the MES cells also featured a significant quantity of the chain-elongating bacterium *Megasphaera sueciensis*. Initial microbial conversion of H_2 and CO_2 in the cells was most likely carried out by a so-far undescribed representative of the *Bacillota* BRH-c20a clade. Overall, this study demonstrates that by combining advanced cathode materials, such as Fe-Sn bimetallic oxide, with a specialized bioaugmented microbial consortium, a high rate of butyrate and caproate production from CO_2 can be achieved.

Received 22nd December 2025
Accepted 23rd February 2026

DOI: 10.1039/d5ra09906d

rsc.li/rsc-advances

1. Introduction

Microbial electrosynthesis (MES) has emerged as a promising carbon capture and utilisation technology for the bioelectrochemical conversion of CO_2 into value-added chemicals.[1] MES uses electroactive (cathodophilic) microorganisms to catalyze the reduction of CO_2 using electrons supplied by a cathode. Compared to electrochemical and thermochemical CO_2 reduction processes, MES operates under milder temperature and pH conditions. Furthermore, the faradaic and CO_2 conversion efficiencies of MES cells are significantly higher. Most interestingly, MES enables the integration of CO_2 reduction with microbial chain elongation to produce upper chain fatty acids (UCFAs), such as butyric and caproic acids, which are used in various applications including chemical precursors for antimicrobial agents, bioplastics, biofuels and food additives.[2,3]

Despite its potential, MES faces several challenges that limit process scale-up. Key limitations include low current density, slow bioreaction rates, and a broad spectrum of products resulting from the metabolic diversity of mixed microbial communities commonly used in MES cells. Recent attempts to address these limitations include studies dedicated to optimizing cathode materials[4–8] and developing microbial populations capable of efficient electron transfer and improved product specificity.[9–11] In this context, the development of biocompatible and highly conductive cathode materials, such as carbon-based electrodes modified with metal oxides, has shown promise in improving biofilm formation and electron transfer efficiency.[12–15]

In addition to cathode material selection, the composition of the microbial community plays a crucial role in determining MES performance. Strategies such as bioaugmentation in which specific microbial strains are introduced, have been explored to enrich acetogenic populations and suppress methanogenic activity, thereby enhancing the production of target compounds, like acetate and UCFAs.[16–22] Introducing a pure strain of chain-elongating bacteria to a mixed acetogenic population can improve chain elongating efficiency and product yield, as the newly introduced strain might have higher specificity for elongation pathways, leading to more consistent and predictable production of UCFAs.[22] The resulting bioaugmented microbial community may become more efficient, with enhanced key metabolic functions. However, the introduced

[a]*École Polytechnique de Montréal, 2500 Ch. de Polytechnique, Montréal, QC H3T 1J4, Canada*

[b]*National Research Council of Canada, 6100 Royalmount Ave., Montreal, Quebec H4P 2R2, Canada. E-mail: Boris.Tartakovsky@cnrc-nrc.gc.ca*

strain could disrupt syntrophic interactions essential for CO_2 conversion, thereby disturbing the natural microbial population balance. Additionally, maintaining the added strain under mixed-culture conditions requires careful control of operating conditions (*e.g.*, pH) and nutrient availability to sustain its desired activity. As a result, the activity of the acetogenic population may be negatively affected. Overall, the success of bioaugmentation is not guaranteed, as it strongly depends on the compatibility of the introduced strain with the existing microbial community and the operational conditions of the MES system.[23]

Our recent study has shown the positive impact of an Fe-Sn bimetallic oxide cathode on the reduction of CO_2 to fatty acids, especially butyrate and caproate, by an acetogenic enrichment.[14] To further improve MES performance, the present study investigated bioaugmentation of this enrichment with *Clostridium kluyveri*.[24] Unlike other members of the genus *Clostridium*, *C. kluyveri* lacks the genetic repertoire for CO_2 fixation *via* the Wood–Ljungdahl pathway and, therefore, cannot grow autotrophically using H_2 and CO_2 as sole substrates.[25] Although frequently detected in MES systems targeting UCFA production,[22,26] its role in these systems is typically restricted to chain elongation, as it cannot obtain electrons directly from the cathode.[27] Importantly, *C. kluyveri* requires both ethanol and acetate as substrates for growth and energy generation, carrying out reverse β-oxidation that converts these precursors to butyrate and caproate.[28] By integrating advancements in cathode material design, particularly Fe-Sn bimetallic oxide coating, and microbial community engineering, this study aims to contribute to the optimization of MES systems for efficient and selective CO_2 conversion to UCFAs.

2. Materials and methods

2.1. MES setup and operating conditions

Three MES cells were operated (MES1, MES2 and MES3), each with a 180 mL cathode compartment volume and a 50 mL anode compartment volume. The cells had a flat plate design with the anode and cathode compartments separated by a Nafion® 211 membrane (Nafion 211, IonPower, Tyrone, PA, USA) with a surface area of 35 cm^2. The membrane was covered by nylon cloth on both sides to provide protection from accidental damage during electrode installation, as described elsewhere.[29] All MES cells used Fe-Sn bimetallic oxide (FeSnO)-coated carbon felt cathodes and Ti/mixed metal oxide mesh anode as described in detail previously.[14] Each cathode consisted of 3 carbon felts ($4 \times 4 \times 0.5$ cm) with a total area of *ca.* 100 cm^2. The cells were operated with a continuous supply of catholyte and anolyte solutions, and gaseous CO_2. The catholyte was continuously supplied using a 50 mL syringe pump at a flow rate of 10 mL per day, while the anolyte solution was fed by a peristaltic pump at an average flow rate of 22 mL per day. Catholyte fed to MES2 and MES3 cells contained variable ethanol concentrations as specified in Table 1.

Catholyte pH was maintained at 6 ± 0.1 for MES1 and at 6.5 ± 0.1 for MES2, MES3 cells using a pH probe installed in the external recirculation loop, a pH controller, and a peristaltic pump, which added 2–5 mL per day of 0.5 M phosphoric acid. Based on the catholyte and pH control streams, an average retention time (HRT) of 13 ± 1 day was maintained in the cathode compartments of all MES cells. The catholyte temperature was maintained at 32.5 ± 1 °C by a temperature controller using a rope heater attached to the external recirculation loop and a temperature probe placed inside the cathode compartment. Gaseous CO_2 was continuously supplied into the cathode compartment through a sparger using a peristaltic pump. Additionally, H_2 was supplied during the startup phase to obtain a H_2/CO_2 ratio of 4 : 1.

The MES cells were operated in constant current mode using a power supply (DC Power supply, PW18–1.8AQ, TEXIO Kenwood, Japan). MES1 was inoculated with 100 mL of an acetogenic enrichment described below. For MES2 and MES3, the same acetogenic enrichment was bioaugmented with *C. kluyveri* culture at approximately 25% of the total inoculum volume. The MES2 and MES3 cells were started after the completion of the MES1 cell and were operated under identical conditions to evaluate the reproducibility of the bioaugmentation approach. Table 1 summarizes the phases of operation for all MES cells, including the corresponding H_2, ethanol, and CO_2 flow rates, and the applied current.

Table 1 Phases and operating parameters of MES cells

MES cell	Phase		Interval (day)	Current		CO_2 (mL d^{-1})	H_2 (mL d^{-1})	Ethanol (mg (L_c d)$^{-1}$)
				mA	A m^{-2}			
MES1	Acclimatization	1	0–8	0	0	200	800	0
	Switch to current supply	2	8–15	30	3.1	200	0	0
	Ramp-up of CO_2 and current supply	3	15–22	50	5.2	200	0	0
		4	22–29	50	5.2	300	0	0
		5	29–45	80	8.3	300	0	0
MES2 and MES3	Acclimatization	1	0–8	0	0	200	800	300
	Switch to current supply	2	8–15	50	5.2	300	0	300
		3	15–22	50	5.2	300	0	0
	Ramp-up of CO_2 and current supply	4	22–34	80	8.3	300	0	0
		5	34–50	80	8.3	300	0	900
		6	50–59	120	12.5	400	0	900
		7	59–69	140	14.6	500	0	900

2.2. Microbial enrichment and pure culture preparation

A mixed microbial enrichment containing acetogenic and chain elongating microorganisms was used as an inoculum. This enrichment was developed using anaerobic sludge originating from an anaerobic digester treating agricultural food waste (Lassonde Inc, Rougemont, QC, Canada) and sludge from a laboratory-scale settler treating food waste collected in Montreal (QC, Canada) as described previously.[14] The enrichment was maintained at 35 °C on a rotary shaker in 120 mL serum bottles with H_2/CO_2 headspace. The bottle headspace was flushed with H_2/CO_2 (80 : 20 vol/vol) once a week. To maintain the mixed microbial consortium of acetogenic and chain elongating bacteria, the culture was transferred to a new set of bottles containing P7 growth medium (pH 6.0) once a month.

A culture of *C. kluyveri* DSM 555 obtained from the Leibniz Institute DSMZ (Braunschweig, Germany) was used to bioaugment the acetogenic inoculum of the MES2 and MES3 cells. A 60 mL serum bottle of this culture was carefully maintained in a Brunswick shaker incubator at 35 °C, with continuous agitation at 120 rpm to ensure optimal growth conditions and metabolic activity. A volume of 20 mL of this culture was added under a biological hood to 100 mL of *C. kluyveri* medium then flushed with N_2/CO_2 (80 : 20 vol/vol) for 5 min. The 500 mL serum bottles were placed in a Brunswick shaker at 35 °C with shaking at 120 rpm. P7 and *C. kluyveri* culture media composition are provided in SI.

2.3. Electrochemical measurements

Electrochemical characterization, including voltammetry and electrochemical impedance spectroscopy (EIS), was conducted using a CHI 760C potentiostat (CH Instruments, Bee Cave, TX, USA). Data acquisition and analysis were performed with the CHI version 20.01 software. An Ag/AgCl (+0.199 V *vs.* reversible hydrogen electrode, RHE, CH Instrument, Bee Cave, TX, USA) electrode was inserted into the cathode compartment during electrochemical characterization and served as a reference, while a dimensionally stable anode located in the anode compartment was used as a counter-electrode.

2.4. Analytical methods and calculations

The composition of the cathode and anode off-gas of the MES cells was analyzed using a gas chromatograph (HP 6890 C, Hewlett Packard, Palo Atlo, CA, USA). Volatile fatty acids (VFAs) and alcohols were also analyzed by gas chromatographs (Agilent 6890 N, Santa Clara, CA, USA) and (Agilent 6890 N, Wilmington, CA, USA), respectively. Method details can be found elsewhere.[30] The flow rate of the cathode compartment off-gas was measured using gas flowmeter (MilliGascounter, PMMA, Ritter, Germany). Dissolved CO_2 concentration was measured by a headspace method after sample acidification as described in the SI.

The catholyte solution consisted of mineral compounds, trace metals, vitamins, and yeast extract. A 0.05 M potassium phosphate solution was used as the anolyte. Detailed composition of all solutions is provided in the SI.

Coulombic efficiency (CE) was calculated as:

$$\mathrm{CE}(\%) = \frac{F\sum_j(\chi_j \times n_j)}{F \times \chi_E \times n_E + \int_t^{t+1} I\,dt} \times 100, \quad (1)$$

where F is the Faraday constant (9 84 851 C mol^{-1}), χ_j is the amount of chemical j (mol) (χ_E corresponds to ethanol), n_j is the number of electrons required for the production of j-th chemical (n_E corresponds to ethanol) from CO_2, and I is the current.

Production rates (P, in mg $(L_c\ d)^{-1}$) of each measurable VFA were calculated based on their concentrations in the anode and cathode compartments and the corresponding liquid flow rates for each compartment.

$$P_j = \frac{C_{c,j}Q_c + C_{a,j}Q_a + \Delta C_{c,j}V_c + \Delta C_{a,j}V_a}{V_c}, \quad (2)$$

where $C_{c,j}$ and $C_{a,j}$ are the concentrations of jth VFA in the cathode and anode compartments, respectively (mg L^{-1}); Q_c and Q_a are the flow rates of the catholyte and anolyte, respectively (L d^{-1}); V_c and V_a are the cathode and anode compartment volumes (L); $\Delta C_{c,j}$ and $\Delta C_{a,j}$ are the concentration difference between two last measurements of jth VFA in the cathode and anode compartments, respectively.

VFA production selectivity (S_e) was defined as the fraction of total electrons used for the production of a specific VFA relative to the total number of electrons in VFAs:

$$\mathrm{Se}(\%) = \frac{\chi_j n_j}{\sum_j(\chi_j n_j)} \times 100 \quad (3)$$

where χ_j is the amount of j-th VFA (mol), n_j is the number of electrons required for production of j-th VFA from CO_2.

The CO_2 removal efficiency (E_{CO_2}) was calculated as follows:

$$E_{CO_2} = \frac{F^{in}_{CO_2} - F^{cat}C_{CO_2} - C^{aq}_{CO_2}}{F^{in}_{CO_2}} \times 100, \quad (4)$$

where $F_{CO_2}{}^{in}$ is the flow rate of pure CO_2 supplied to the cathode (mL d^{-1}), F^{cat} is the cathode off-gas flow (mL d^{-1}), $C_{CO_2}{}^{aq}$ is dissolved CO_2 in solution (mL d^{-1}), and C_{CO_2} is the fraction of CO_2 in the cathode off-gas.

2.5. Microbial community analysis

The acetogenic inocula, the catholytes, and the cathodic biofilms samples were kept frozen at −30 °C until biological analysis. Microbial genomic DNA was extracted using the DNeasy PowerLyzer PowerSoil Kits from Qiagen (Hilden, Germany) following the manufacturer's guide. Genomic DNAs were quantified using the Qubit 1X dsDNA HS assay kit (ThermoFisher Scientific). Microbial community of the samples was characterized by amplicon sequencing of nearly full-length 16S rRNA genes, amplified using the primers 27F (5′-AGRGTTYGATYMTGGCTCAG-3′)[31] and 1492R (5′-RGYTACCTTGTTACGACTT-3′).[32] Amplicons were sequenced by Circular Consensus Sequencing (CCS) on a PacBio sequencing platform. Amplicon generation and sequencing were carried out at the Integrated Microbiome Resource facility (Dalhousie

University, Canada). Amplicon sequences were analyzed following the longread workflow of the DADA2 pipeline (version 1.32).[33] Amplicon sequence variants (ASVs) generated through the pipeline were taxonomically classified using the dada2-internal implementation of the RDP Naive Bayesian Classifier,[34] and using representative 16S rRNA gene sequences of the SILVA database (NR99 v138.2;[35]).

Downstream analyses of ASV count tables were carried out in R (v4.4.1; https://www.r-project.org) using (i) the tidyverse package read (v2.1.5 and v1.3.1),[36] and the Bioconductor (https://www.bioconductor.org) package ShortRead (v1.62.0)[37] for data wrangling; and (ii) the tidyverse package ggplot2 (v2.5.2) for visualizing prominent ASVs. The obtained ASVs were aggregated at the species level using PhyloSeq (v1.48.0)[38] using prior to data analysis.

The sequencing data for this study have been deposited in the European Nucleotide Archive (ENA) at EMBL-EBI under accession number PRJEB106961 (https://www.ebi.ac.uk/ena/browser/view/PRJEB106961).

The catholytes of MES2 and MES3 were periodically sampled to quantify the *C. kluyveri* population by droplet digital PCR (ddPCR). To this end, genomic DNA was extracted and quantified as before. ddPCR reactions were prepared with primers targeting *C. kluyveri* (forward: 5′-CAAGCCTGGTAGTTGATACG-3′; reverse: 5′-TTAAAGGCCCTCTGTACTCC-3′),[39] along with ddPCR supermix (BioRad Laboratories), and DNA templates. Reactions were partitioned into droplets using QX200 droplet generator, followed by thermal cycling under standard cycling conditions (initial denaturation at 95 °C for 5 min followed by 40 cycles of 95 °C for 30 s, 59 °C for 60 s, 72 °C for 30 s; cooling at 4 °C for 5 min followed by a final extension at 90 °C for 5 min then a 4 °C hold; ramp rate = 50% (2 °C s^{-1})). Droplets were read using the QX200 Droplet Digital reader, and data was analyzed with QuantasoftTM software (Bio-Rad) to determine the absolute abundance of *C. kluyveri* genome copies on Poisson statistics. Additional details are provided in SI.

3. Results and discussion

3.1. Impact of CO_2 flow and applied current

Throughout the experiments, the impacts of CO_2 flow and applied current were investigated by a stepwise increase of the CO_2 inflow and a simultaneous increase in the applied current to provide a sufficient supply of electrons for microbial metabolic activities leading to CO_2 reduction to VFAs (Table 1). The experiments were carried out in distinct phases. Immediately after inoculation, H_2 (800 mL per day) and CO_2 (200 mL per day) were supplied to all MES cells to serve as sources of electrons and inorganic carbon, respectively, and promote initial microbial growth (Phase 1). During this acclimation and biofilm growth phase, the current was set to zero. In Phase 2, a current was applied to all MES cells, replacing H_2 as the electron donor. For MES1, the current density was fixed at 3.1 A m^{-2} and the CO_2 flow rate was maintained at 200 mL per day. In Phases 3–5, the current was gradually increased to 8.3 A m^{-2} and the CO_2 flow rate was increased to 300 mL per day. Such gradual stepwise increase in CO_2 supply and applied current was implemented to allow the acetogenic enrichment inoculum to gradually adapt to the changing cathodic conditions, where the cathode provides electrons and H_2, and avoid inhibition of acetogenic and chain-elongating microbial activity by excessive cathode potential and high concentrations of dissolved CO_2 and H_2.[40] This approach also enabled the evaluation of steady-state performance at the end of each phase, facilitating the analysis of product selectivity in relation to operating conditions.

For MES2 and MES3, based on the fast adaptation to current during Phase 1 observed for MES1 (which was operated earlier), the current density was set to 5.2 A m^{-2} and the CO_2 flow rate to 300 mL per day (Phase 2). The current and CO_2 flow rate were then gradually increased reaching 14.6 A m^{-2} and 500 mL per day, respectively in Phase 7. In contrast to MES1, MES2 and MES3 were fed with ethanol during Phases 1, 2 and then Phases 5–7 to support chain-elongation by *C. kluyveri*. The impact of ethanol and *C. kluyveri* on VFA production will be discussed later. Notably, the MES1 inoculum was not bioaugmented with *C. kluyveri* and this cell was not provided with ethanol, as it was intended to be used as a "negative control" to evaluate the impact of this chain-elongating strain on butyrate and caproate formation and assess whether the native microbial community alone could accomplish CO_2 reduction and chain elongation to caproate. Thus, MES1 provided a baseline for comparison with MES2 and MES3.

In the absence of current, the CO_2 consumption rate was low for all three MES cells (<60%; Fig. 1A). For MES1, when current was applied and the CO_2 flow rate was set to 200 mL per day (1.11 L $(L_c\ d)^{-1}$), over 90% CO_2 was consumed, corresponding to a CO_2 consumption rate of 1.0 L $(L_c\ d)^{-1}$. However, CO_2 consumption decreased to 86% when the CO_2 flow rate was increased to 300 mL per day (1.67 L $(L_c\ d)^{-1}$) and the current density was increased to 8.3 A m^{-2} (Phase 5). This decrease in CO_2 removal suggests that under these operating conditions the maximum rate of CO_2 uptake for MES1 had been reached, corresponding to 1.43 L $(L_c\ d)^{-1}$), and that CO_2 reduction became limited by microbial metabolism.

It should be noted that CO_2 transfer to liquid could also have limited its rate of uptake. Indeed, dissolved inorganic carbon (CO_2 and carbonate) measurements (detailed method description provided in SI) showed low concentration (<0.2 g L^{-1}) of inorganic carbon in liquid at all tested CO_2 flow rates and in all MES cells. Such low concentration can be attributed to fast CO_2/carbonate consumption by acetogenic bacteria. At the same time, as will be emphasized later in the discussion, higher CO_2 uptake rates were observed for MES2 and MES3, while dissolved CO_2 and bicarbonate concentrations were similar, thus suggesting that microbial metabolism was the main limiting factor in CO_2 uptake. For MES2 and MES3, the CO_2 consumption rate was relatively higher (1.57 L $(L_c\ d)^{-1}$) at a flow rate of 300 mL per day and current density of 8.3 A m^{-2}. However, the CO_2 removal efficiency decreased from 94% to 85% (2.36 L $(L_c\ d)^{-1}$) at the highest CO_2 inflow rate of 2.78 L $(L_c\ d)^{-1}$ (500 mL per day), indicating a similar limitation due to bacterial activity. Nevertheless, this CO_2 uptake rate was 14% higher than that of MES1.

The coulombic efficiency (CE) was calculated for each phase of operation of the MES cells except for Phase 1 during which no

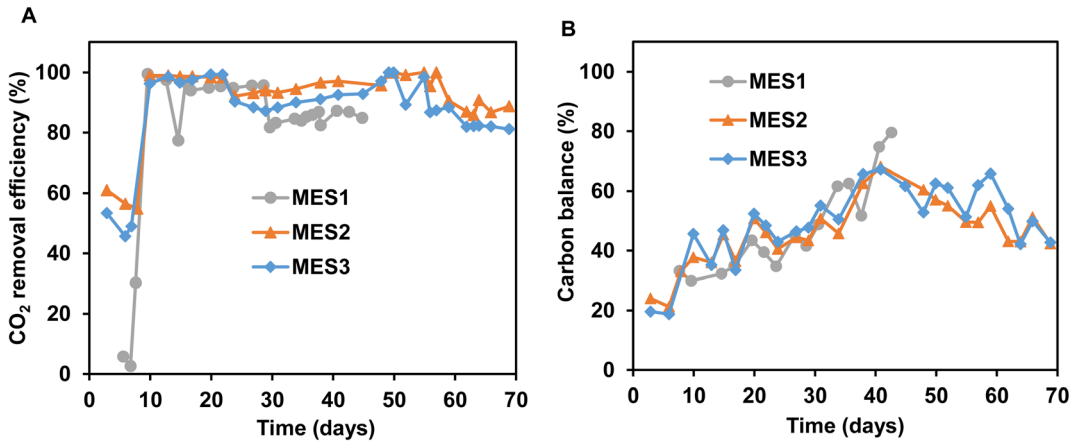

Fig. 1 (A) CO_2 removal efficiency and (B) carbon balance in the MES cells under different operating conditions.

current was applied (Fig. 2). These calculations took into account the electrons supplied by the ethanol for MES2 and MES3 operation. During the operation phases 2 and 3 of MES1 (Fig. 2A), the coulombic efficiency remained relatively low (60 ± 6% and 63 ± 1%, respectively). CE values increased during the following two operational phases, reaching 88 ± 1% in the final Phase 5, while the CO_2 consumption rate decreased during this phase, as mentioned above. Additionally, the corresponding VFA carbon balance showed less than 50% carbon recovery (Fig. 1B), suggesting that other unmeasured compounds may have been produced.

Since MES2 and MES3 demonstrated above 90% CO_2 consumption at a CO_2 supply of 300 mL per day, the CO_2 flow and current density in Phase 7 were increased to 500 mL per day (2.78 L $(L_c\ d)^{-1}$) and 14.6 A m^{-2}, respectively. Overall, MES2 and MES3 showed similar performance, with minor differences observed during Phases 2 (days 8–15) and 4 (days 22–34) (Fig. 2B and C). The coulombic efficiencies of these cells were relatively higher compared to MES1 at the same operating conditions. During operation phases 3 and 4, MES2 and MES3 were maintained at current densities of 5.2 A m^{-2} and 8.3 A m^{-2} (CO_2 flow of 300 mL per day) and with no external ethanol supply. These operating conditions correspond to phases 4 and 5 of MES1 (Table 1). CE values of MES3 during Phases 3 and 4 were 99 ± 6% and 99 ± 10%, respectively, while corresponding CE values (Phase 4 and 5) for MES1 were lower (82 ± 2% and 88 ± 2%, respectively). However, when the current density was increased to 12.5 A m^{-2} (120 mA) (days 50–59; Fig. 2B and C), a significant CE decrease was observed suggesting that microbial metabolic activity is not always proportional to the applied current density or that unidentified compounds were produced based on the low value of carbon recovery (<66%, Fig. 1B).

3.2. Distribution of VFAs

The measurable CO_2 reduction products included alcohols and VFAs in the anolyte and catholyte effluent streams. Based on analytical measurements, nearly 50% of all produced compounds were recovered in the anolyte, indicating significant diffusion of CO_2 reduction products through the Nafion membrane, most likely due to VFA concentration and pH gradients. Indeed, the anolyte pH of 1.5–2 might lead to VFAs protonation near the membrane thus increasing the transport of undissociated molecules. Since the acetogenic enrichment used to inoculate the MES cells did not contain detectable methanogenic populations, CH_4 was not detected in the cathode off-gas, while C2–C6 VFAs represented the majority of recovered products, as demonstrated by the CE calculations (Fig. 2). Measured alcohol concentrations were low (including methanol, ethanol, propanol, butanol, *tert*-butanol), always below 80 mg L^{-1}, although actual production may have been higher due to rapid bacterial consumption. Therefore, alcohol production was not included in the electron efficiency calculations. H_2 was generated in all MES cells. The coulombic efficiency corresponding to the hydrogen released from the cathode compartment generally increased with current density but remained low compared to that of VFAs (Fig. 2).

VFA production showed an increasing trend during almost all phases of operation of the MES1, MES2, and MES3 cells (Fig. 3). This suggests that in response to increasing CO_2 and current supply, microbial activity increased both in the cathodic biofilm and the catholyte. In MES1, VFA production was low (<100 mg $(L_c\ d)^{-1}$) after inoculation. Acetate production gradually increased from the start of current application, reaching a peak of 1145 mg $(L_c\ d)^{-1}$. This highlights the impact of current (electron availability) on microbially catalyzed CO_2 reduction. After day 22 (Phase 3), the measured acetate concentration and, accordingly, acetate production decreased over time, while butyrate production, initially low, significantly increased. A maximum production rate of 875 mg $(L_c\ d)^{-1}$ was achieved on day 45 (Phase 5), indicating that chain-elongating microorganisms, which proliferated in the bulk liquid and cathodic biofilm, utilized acetate to produce butyrate (Fig. 3A). Subsequently, caproate production increased suggesting the conversion of butyrate into caproate through the chain elongation process.[41] A maximum caproate production of 94 mg $(L_c\ d)^{-1}$ was reached on day 43 (Phase 5).

Coating of carbon-based materials is a promising approach for improving the charge transfer of biocathodes as well as the

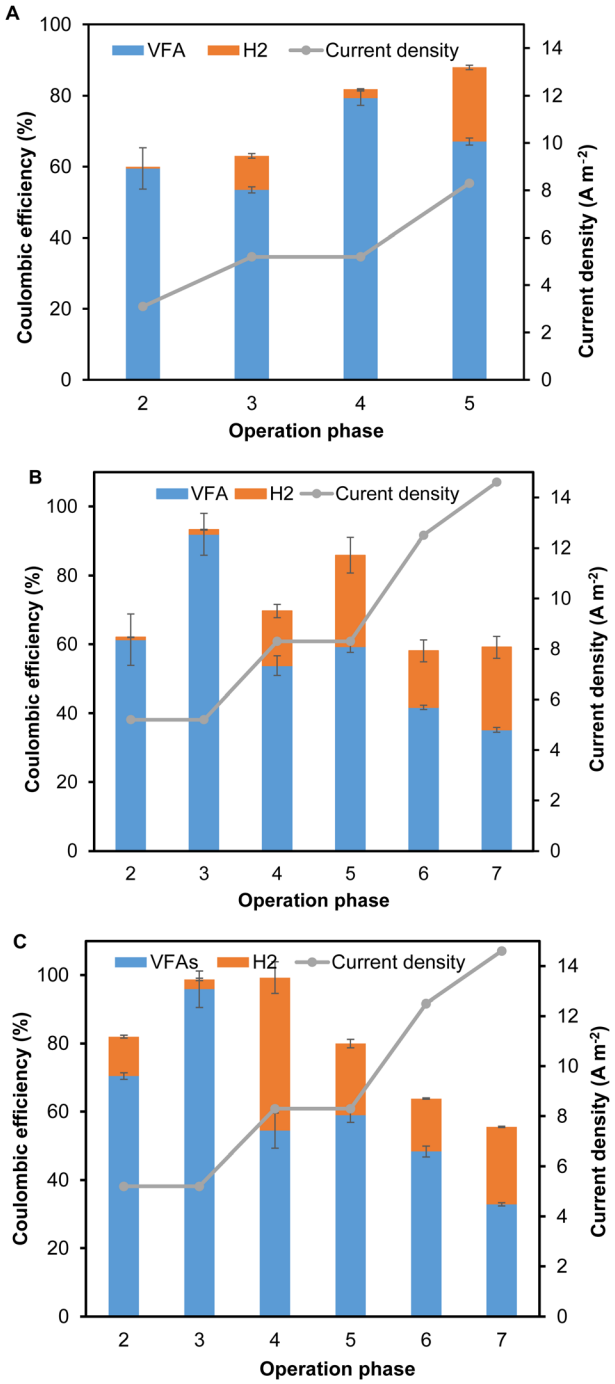

Fig. 2 Coulombic efficiency of (A) MES1, (B) MES2 and (C) MES3 in different operating conditions. Error bars show standard deviation of periodic analysis.

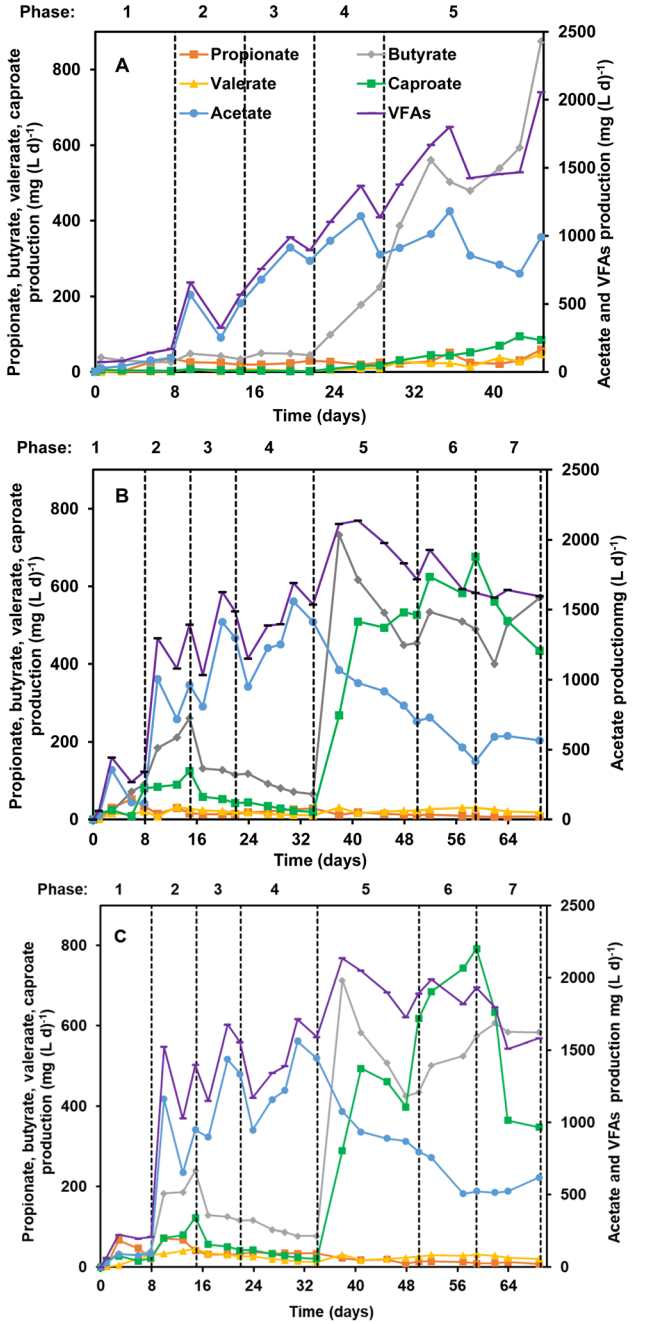

Fig. 3 Production of VFAs in (A) MES1, (B) MES2 and (C) MES3 under different operating conditions.

selectivity of reaction products. Several studies have demonstrated the positive impact of modifying carbon supports with various metal-based materials (CuO/g-C_3N_4/rGO, Fe_x,MnO_y, Mo_2C/N, TiO_2, MnO_2) on the bioelectrochemical reduction of CO_2 by mixed microbial consortia to VFAs, especially acetate.[42–46] Additionally, an engineered *Clostridium ljungdahlii* used in MES cell with a Ni–P coated cathode was shown to enhance butyrate production.[47] The achieved butyrate production in that work was 100 mg (L d) $^{-1}$, which is much lower than that of MES1 (875 mg (L_c d)$^{-1}$) of the current study. Another study demonstrated that coating a carbon felt cathode with a bimetallic oxide $NiFe_2O_4$ in a MES cell, improves butyrate selectivity from 37% to 95%.[15] The associated butyrate production with this cathode was 191.5 mg (L_c d)$^{-1}$, which is still lower compared to the performance of MES1.

The FeSnO catalyst played a crucial role in facilitating both electrochemical and bioelectrochemical reactions in the MES2 and MES3 cells. Under abiotic conditions, FeSnO primarily catalyzed H_2 production, while after inoculation with the

acetogenic enrichment it enhanced electron transfer between the cathode and the electroactive biofilm. This improved electron flow supported acetogenic activity, leading to efficient acetate formation and chain elongation. Overall, FeSnO not only promoted H_2 evolution, but also accelerated bioreaction rates by facilitating the interaction between the electrode and microbial cells, *e.g.* through reduced activation looses.

The trends of VFA production in MES2 and MES3 differed from those of MES1 (Fig. 3B and C). Similar to MES1, after current application acetate production rate rapidly increased to 1559 mg $(L_c\ d)^{-1}$ and 1561 mg $(L_c\ d)^{-1}$ in MES2 and MES3, respectively. Unlike MES1, the production rate of butyrate and caproate increased simultaneously suggesting efficient acetate chain elongation by *C. kluyveri*, using ethanol as an electron donor.[28,48] From day 15 (end of Phase 2), ethanol addition was stopped, causing a sharp decrease in butyrate and caproate production and confirming that, as expected, ethanol was the main electron donor for acetate conversion by *C. kluyveri*. Compared to similar phases during the operation of MES1, butyrate and caproate production remained low in the absence of ethanol despite an increase in current density to 8.3 A m^{-2}. Upon resumption of ethanol feeding at a higher flow rate (900 mg $(L_c\ d)^{-1}$), in Phase 5 (days 34–50), butyrate and caproate production rapidly increased. The butyrate production rate reached 733 mg $(L_c\ d)^{-1}$ in MES2 and 713 mg $(L_c\ d)^{-1}$ in MES3 by day 38. Subsequently, caproate production rate peaked at the end of Phase 6 (day 59), reaching 676 mg $(L_c\ d)^{-1}$ in MES2 and 792 mg $(L_c\ d)^{-1}$ in MES3. Importantly, in both cells ethanol feed did not affect the rate of CO_2 uptake. By the end of the last operational Phase 7, corresponding to a current density of 14.6 A m^{-2}, the caproate production rate decreased, while the butyrate production rate minimally increased. Also, acetate production (and therefore steady-state concentration) somewhat increased.

3.3. The impact of bioaugmentation with *C. kluyveri* and of ethanol addition on butyrate and caproate production

In the MES1, acetate was the main VFA produced during the first 29 days of operation (Phases 1–4). Subsequently, increased chain elongation was observed between days 29–45 (Phase 5), where the production rate of butyrate and caproate reached 875 mg $(L_c\ d)^{-1}$ and 94 mg $(L_c\ d)^{-1}$, respectively. The corresponding average selectivities for butyrate and caproate were estimated at 49 ± 2% and 9 ± 2%, respectively. Also, the maximum ethanol concentration observed during this period was 72 mg L^{-1}. Phase 5 corresponded to MES1 operation at an increased current density of 8.3 A m^{-2} (Table 1). It can be hypothesized that in this phase ethanol produced through solventogenesis from acetate and/or electrochemically from CO_2 was used as an electron source for the conversion of acetate to butyrate and caproate.

The impact of bioaugmentation with *C. kluyveri* and ethanol addition on CO_2 reduction to butyrate and caproate was assessed during the operation of MES2 and MES3. Unlike MES1, butyrate and caproate production was already significant from the start of the MES2 and MES3 operation (Phases 1 and 2). However, when the ethanol supply was stopped (Phases 3 and 4), the concentrations and therefore the production of these VFAs immediately declined. Accordingly, during Phase 4 (days 22–34), the production rates of butyrate and caproate in MES2 and MES3 were lower than in MES1. This decline suggests that

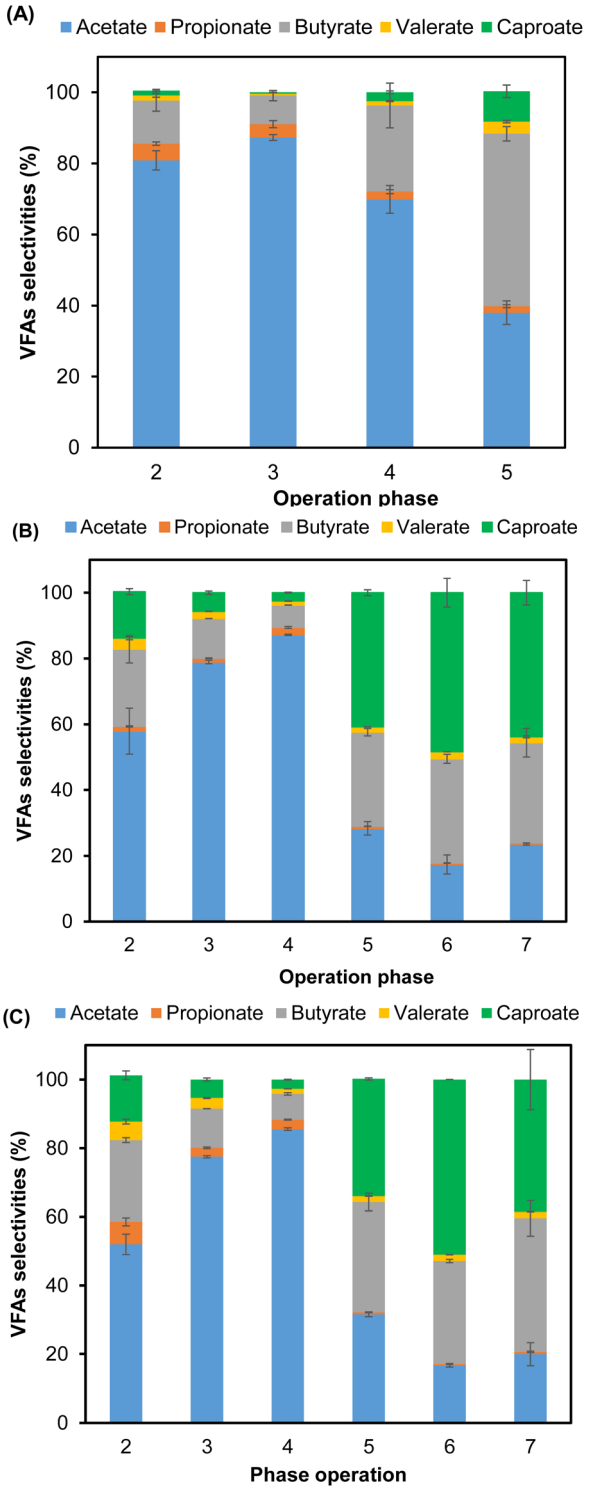

Fig. 4 Selectivity of VFAs in (A) MES1, (B) MES2 and (C) MES3 experiments under different operating conditions.

the chain elongating microbial populations in MES1 evolved to be less dependent on ethanol. In the absence of ethanol supplied to MES2 and MES3, the population of *C. kluyveri* declined compared to its initial density (Fig. 5), confirming its dependence on exogeneous ethanol. These observations indicate that ethanol production by the mixed acetogenic consortium and/or through the electrocatalytic activity of the FeSnO cathode coating was insufficient to sustain the metabolic activities of *C. kluyveri*. At the same time, chain-elongating bacteria within the mixed microbial consortium were likely better adapted to low ethanol availability and/or capable of using the cathode as an electron source,[26] although these populations had lower efficiency.

To support growth and metabolic activity of *C. kluyveri*, between days 34–69 (Phases 5–7), ethanol supply to MES2 and MES3 resumed at a load of 900 mg $(L_c\ d)^{-1}$, resulting in increased chain elongation activity and, consequently, higher concentrations of butyrate and caproate. Also, based on ddPCR monitoring of catholyte, proliferation of *C. kluyveri* was confirmed throughout these phases (Fig. 5). Notably, caproate production in MES2 and MES3 increased 6 and 5-fold, respectively, compared to a similar period of MES1 operation (days 29–45). The highest average selectivities were achieved during Phase 7 (days 50–59) and were estimated at 32 ± 1% (butyrate) and 48 ± 4% (caproate) for MES2, and 30 ± 1% (butyrate) and 51.0 ± 0.1% (caproate) for MES3 (Fig. 4B and C). However, the CE calculated for VFA production remained below 50% (Fig. 2B and C). During phase 7 (days 59–69), the caproate production rate was decreasing, while the acetate production rate was increasing. Considering the progressively increasing density of *C. kluyveri*, which has been shown to also produce caprylate,[49] caproate conversion into caprylate (C8 fatty acid) can be hypothesized.[49] However, analytical methods used in this study did not include caprylate measurements. A decrease in caproate production when the cathode potential changed from −1 V to −1.1 V/Ag/AgCl has been previously demonstrated[40] and can explain a lower caproate concentration in Phase 7. Similar results were also obtained in another study at a more negative potential of −1.2 V *vs.* Ag/AgCl.[50] At a current density of 14.6 A m^{-2} (Phase 7), a cathodic potential of −1.29 ± 0.03 V *vs.* Ag/AgCl, could either result in decreased caproate production or caproate conversion into caprylate (or both), thus explaining the decrease in caproate production. In this phase, the low CE (<65%) and incomplete carbon balance suggest that reaction products other than C2–C6 VFAs and H_2 were produced by other members of the mixed microbial consortium.

The addition of external electron sources like methanol and ethanol to enhance chain elongation of short and medium chain fatty acids in MES cells has been explored in various studies. The conversion of CO_2 and ethanol into caproate in a MES cell using mixed microbial consortium and a carbon felt cathode has previously been demonstrated. The results showed a caproate production of 2410 ± 690 mg $(L_c\ d)^{-1}$ with a very high selectivity of 91.47 ± 0.58%.[17] However, the CE in this MES cell was low (12.23 ± 0.02%) because of high ethanol utilization. Similarly, another study examined the use of methanol as an additional electron donor in a MES cell to reduce CO_2 using a mixed microbial culture predominantly consisting of *Eubacterium* genus.[51] In this case, butyrate was the main product, reaching a production rate of 360 ± 10 mg $(L_c\ d)^{-1}$. Table 2 provides a summary of VFA production in MES cells with and without supplementary carbon sources reported in different

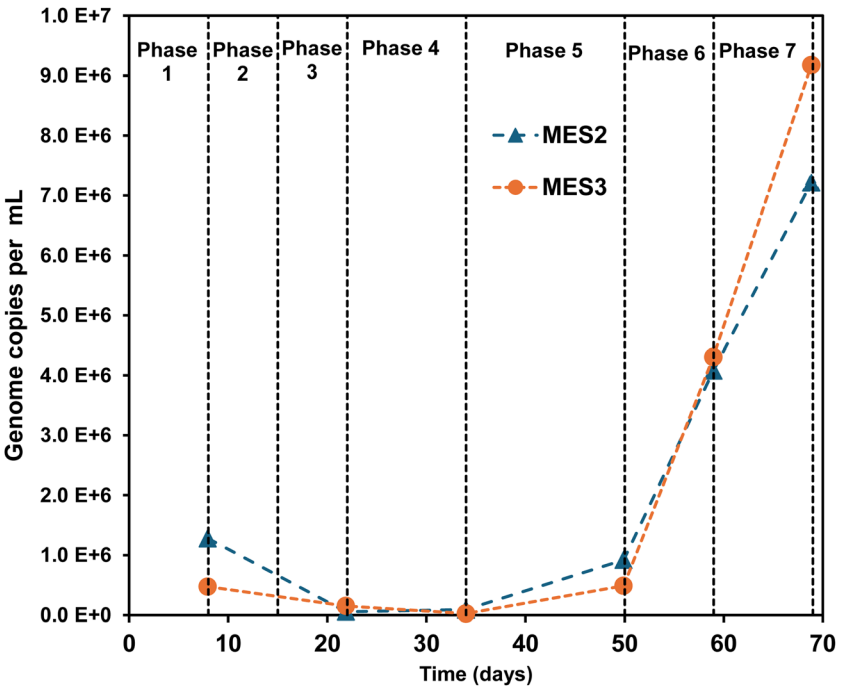

Fig. 5 Number of genome copies of *C. kluyveri* in cathode off liquid of MES2 and MES3 as determined by ddPCR.

published studies and compares these values with those obtained in this study. It can be hypothesized that methanol (or ethanol) produced by electrochemical catalysis on Fe-Sn bimetallic oxide probably contributed to butyrate production in the three MES cells.

3.4. Microbial community analysis

In order to characterize the microbial communities associated with the individual MES cells, the inocula, catholytes and cathode-associated biofilms were collected at the end of the experiment, and were analyzed by 16S rRNA gene amplicon long-read sequencing (Fig. 6).

The enrichment used as inoculum, originally sourced from combined dark-fermentation and anaerobic-digestion sludges, underwent successive transfers in serological bottles under a H_2 and CO_2 atmosphere, promoting a metabolic shift from chemoorganotrophy to chemolithotrophy, and thereby enriching microorganisms capable of carbon dioxide fixation. The resulting microbial community was able to produce significant concentrations of acetate and butyrate, as well as smaller amounts of propionate, valerate, and caproate. This enrichment culture primarily consisted of bacteria classified as *Megasphaera sueciensis* (ASV1; 53%), *Clostridium aciditolerans* (ASV14; 15%), Prevotellaceae sp. (ASV3; 13%), *Clostridium autoethanogenum* (ASV9; 13%) and a minor population of *C. ljungdahlii* (ASV23; 2%). *Megasphaera sueciensis* is a known chain elongator that has been shown to produce butyrate and caproate from acetate.[52,53] *Clostridium aciditolerans* is an acid-tolerant fermentative bacterium that is unable to grow by homoacetogenesis.[54] *Clostridium autoethanogenum* is a well-characterized homoacetogen capable of producing acetate and ethanol from CO_2 and H_2.[55] *C. ljungdahlii*[56] is another homoacetogen with metabolic capabilities similar to those of *C. autoethanogenum*; however, the two species differ in key physiological traits, including the ratios of produced end products.[57,58] The detected Prevotellaceae sp. sequence is most closely affiliated (99.93% sequence identity over a length of 1453 basepairs) with *Segatella asaccharophila* – a species showing enhanced growth in the presence of CO_2 and being capable of producing succinate and acetate by fermentation.[59]

Despite efforts to maintain identical enrichment conditions, the microbial composition of the enrichment culture had somewhat shifted by the time it was used to inoculate the MES2 and MES3 cells, nearly 8 months after the operation of MES1. The relative abundances of *Megasphaera sueciensis* (55%), Prevotellaceae sp. (16%) and *C. ljungdahlii* (1%) remained similar to the initial enrichment culture, however the population of *Clostridium aciditolerans* had been greatly reduced (1%) and *Clostridium autoethanogenum* was no longer detectable. Instead, this evolved enrichment contained a significant proportion of bacteria classified as *Clostridium luticellarii* (ASV7; 21%). *Clostridium luticellarii* is a known chain elongator that has been shown to produce butyrate, isobutyrate, and caproate from methanol and acetate.[60] It is also able to grow on H_2 and CO_2 with acetate and butyrate being the main products, and caproate being produced in trace amounts.[60]

Table 2 Comparison of acetate, butyrate and caproate production in MES cells

Inoculum	Cathode materials	C-source	Current	E_{cath}	VFAs production (mg (Lc d)$^{-1}$)			VFAs titer (mg L^{-1})			Electron recovery	Reference
			A m^{-2}	V	C2	C4	C6	C2	C4	C6	%	
Mixed culture	CuO/g-C_3N_4/rGO-CF	CO_2	−14.8	−0.9	270	—	—	3800 ± 50	—	—	—	43
Enriched mixed culture	Mo_2C/N-LS	CO_2	—	−1.05	150	—	—	6080	—	—	68	42
Enriched mixed culture	TiO_2-CF	CO_2	—	−0.9	2150 ± 150	—	—	8860	—	—	72.76 ± 6.28	46
C. ljungdahlii	Ni–P-CF	CO_2	—	−1.05	1700	100	—	1180 ± 10	670 ± 10	—	81.7	47
Mixed culture	$NiFe_2O_4$-CF	CO_2	−0.14	−0.8	—	191.52	—	50	958	—	—	15
Mixed culture	Graphite granules	CO_2 + methanol	1.3	−1.0	60 ± 20	280 ± 40	—	1300–2100	7000 ± 1000	—	77.2 ± 10.0	51
Raw activated sludge	CF	CO_2 + ethanol	10	—	—	—	2410 ± 690	1150 ± 770	1220 ± 730	7660 ± 1380	12.23 ± 0.02	17
Enriched mixed culture	FeSnO-CF	CO_2	8.3	−0.95	754 ± 46	566 ± 38	89 ± 7	4459 ± 103	2819 ± 137	400 ± 37	88 ± 2	This work (MES1)
Enriched mixed culture	FeSnO-CF	CO_2 + ethanol	12.5	−1.05	515 ± 12	550 ± 34	768 ± 35	2343 ± 46	2845 ± 12	2519 ± 87	64 ± 2	This work (MES3)

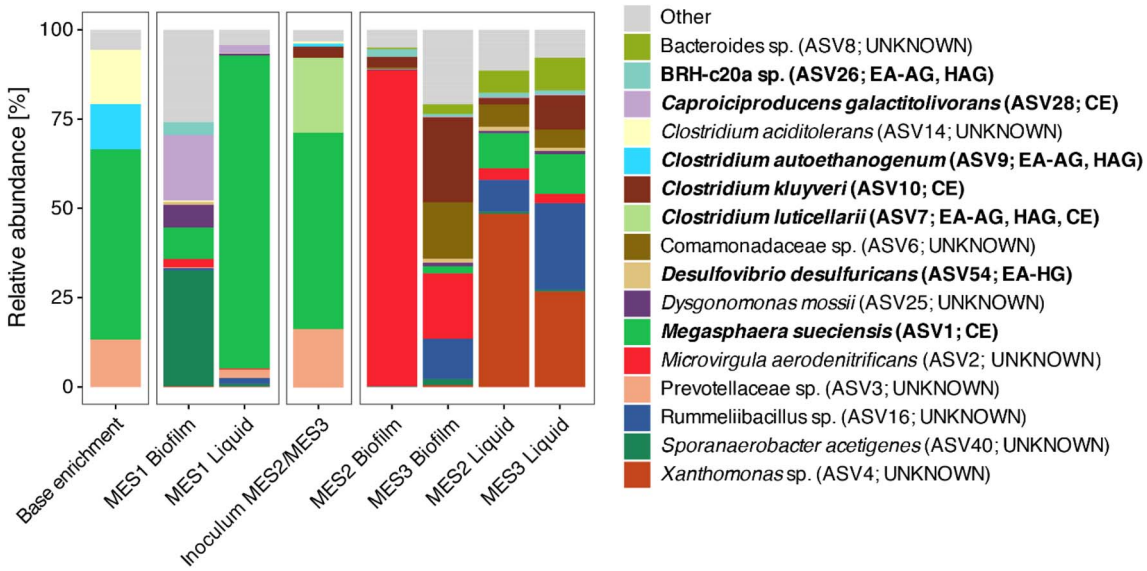

Fig. 6 Relative abundances of the most abundant ASVs (based on the mean abundance across samples) in the base enrichment, the inoculum of MES2/MES3, and the catholyte and biofilm samples. Taxonomic identity of ASVs is color-coded. ASV identifiers and predicted function (EA-AG, electroactive acetogen; EA-HG, electroactive hydrogenogen; HAG, homoacetogen; CE, chain-elongator) within the MES cells are provided in parentheses. ASVs with a function prediction are emphasized in bold print. Please note that the presence of *C. kluyveri* in the inoculum of MES2 and MES3 represents the bioaugmentation.

Of the bacteria dominating the inocula, only *M. sueciensis* thrived under the operating conditions of the MES cells, being detectable in all but one of the collected MES samples, and representing up to 83% of the individual microbial communities (Fig. 6). In addition to *M. sueciensis* already enriched in the inoculum and the bioaugmentation strain *C. kluyveri*, microbial communities at the end of the experiment consisted primarily of bacterial species that were not detectable in the initial inoculum. Furthermore, the composition of the microbial communities varied considerably not only between the bioaugmented MES cells and the control, but also between the two bioaugmented replicates.

At the end of the experiment, the cathodic biofilm of the control MES1 cell was dominated primarily by *Sporanaerobacter acetigenes* (ASV40; 33%), *Caproiciproducens galactitolivorans* (ASV28; formerly Clostridium sp. BS-1; 18%), the aforementioned *M. sueciensis* (9%) and a bacterium identified as *Dysgonomonas mossii* (ASV41; 6%). *Caproiciproducens galactitolivorans* has previously been shown to produce H_2, CO_2, ethanol, acetate, butyrate, and caproate through fermentation of sugars and alcohols.[61] It has also been reported that this bacterium exhibits enhanced growth when co-cultured with ethanol, acetate, and butyrate producers.[61] Based on these observations, it can be hypothesized that *C. galactitolivorans* is capable of producing caproate from ethanol, acetate, and butyrate; however, experimental evidence for this metabolic capability is currently lacking. Representatives of the genus *Dysgonomonas* have previously been detected in other bioelectrical systems[62–64] suggesting that bacteria of this clade are electroactive. However, their exact role in these systems is currently still unknown. Finally, *S. acetigenes* has also previously been suggested to be electroactive[65] and has been associated with ethanol consumption in CO_2-supplemented carboxylate-fed bioreactors.[66] The microbial community of the corresponding catholyte of MES1 consisted primarily of *M. sueciensis* (88%).

The composition of the cathode biofilms between the bioaugmented MES2 and MES3 cells differed considerably despite same operating conditions for both cells. The MES2 biofilm consisted primarily of a bacterium closely affiliated with *Microvirgula aerodenitrificans* (ASV2; 88%) and the added *C. kluyveri* (ASV10; 3%). Both of these bacteria were also present in the MES3 biofilm, albeit with notably different relative abundances: *M. aerodenitrificans* (18%), *C. kluyveri* (23%). Additional noteworthy bacteria detected in the MES3 biofilm include a bacterium identified as *Rummeliibacillus* sp. (ASV16; 11%) and a bacterium identified as *Comamonadaceae* sp. (ASV6; 16%). Representatives of *M. aerodenitrificans*[67] and *Rummeliibacillus* sp.[68] have previously been detected in bioelectrochemical systems, however their exact role in these systems remains unclear. The closest cultured relative of the Comamonadaceae-affiliated bacterium is *Saezia sanguinis*. *S. sanguinis* has been isolated from blood,[69] and there have so far not been any reports regarding the presence of these bacteria in a bioelectrochemical or biotechnological systems.

Despite the significant differences between the cathode biofilms of the MES2 and MES3 cells, the microbial communities of the corresponding catholyte samples were surprisingly similar. Both catholyte samples were dominated by a bacterium affiliated with the Lysobacteraceae SN8 clade (ASV4; relative abundances: MES2, 49%; MES3, 27%), a clade characterized by the presence of *Xanthomonas massiliensis* SN8. Interestingly, this bacterium only represented a negligible portion (<1% relative abundance) of all the other collected samples, and can therefore be considered specific to the catholytes of the two

bioaugmented MES cells. Representatives of the genus *Xanthomonas* are primarily known as plant pathogens,[70] although some representatives have also been detected in engineered systems such as microbial fuel cells[71] or bioreactors.[72] The species *Xanthomonas campestris* has been shown to grow under anaerobic conditions by using extracellular electron transfer mechanisms.[73] Despite this, the role of *Xanthomonas* species in engineered systems currently unknown. Interestingly, while *Xanthomonas* in engineered systems are typically encountered in the form of biofilms,[71,74] the *Xanthomonas* sp. detected in the present study appeared to thrive predominantly in planktonic form. In addition to *Xanthomonas*, the microbial communities of the MES2 and MES3 catholytes consisted primarily of bacterial populations also detected in cathode biofilms, such as *M. aerodenitrificans* (MES2: 3%; MES3: 3%), *Rummeliibacillus* sp. (9%; 24%), *M. sueciensis* (10%; 11%), Comamonadaceae sp. (7%; 5%), and *C. kluyveri* (2%; 10%).

3.5. Microbial production of caproate

Based on a simplified conceptual model for the production of the medium-chain fatty acid caproate (Fig. 7) and the composition of the individual microbial communities, it can be attempted to reconstruct how caproate was produced in the different setups: In the base enrichment culture, *C. autoethanogenum* may have been primarily responsible for the initial conversion of H_2 and CO_2, as suggested by its elevated relative abundance. In the evolved enrichment culture used to inoculate the MES2 and MES3 cells, this initial conversion appears to have been mainly taken over by *C. luticellarii*. Minor populations of *C. ljungdahlii* were detected at both stages and could have contributed to the conversion of H_2 and CO_2 throughout the enrichment process. The acetate, ethanol, and butyrate produced during both stages of the enrichment were most likely utilized by *M. sueciensis* for chain elongation, resulting in the production of caproate. The role of the detected Prevotellaceae sp. in the inoculum remains unresolved.

Notably, acetate conversion to caproate required the presence of ethanol. It can be hypothesized that electrochemical and microbial pathways for ethanol production coexisted (Fig. 7). Electrochemically catalyzed ethanol production is plausible, while acetate conversion to ethanol through solventogenesis is a well-established microbial process, typically involving species such as *C. ljungdahlii* and *Clostridium autoethanogenum*.[75] However, abiotic operation of MES cells demonstrated that electrochemical CO_2 reduction resulted in very low production rates, with ethanol concentration at around 1 mg L^{-1} at a current of 30 mA. Under these conditions electrochemical production of acetate was also observed, yet acetate production was also low with a concentration of 20–45 mg L^{-1}. Based on these results the solventogenesis pathway appears to be the more likely mechanism. Nevertheless, the conceptual model in Fig. 7 includes both electrochemical and microbial pathways of ethanol production.

Desulfovibrio desulfuricans (ASV54) accounted for approximately 1% of the bacterial community in all MES cells. Known

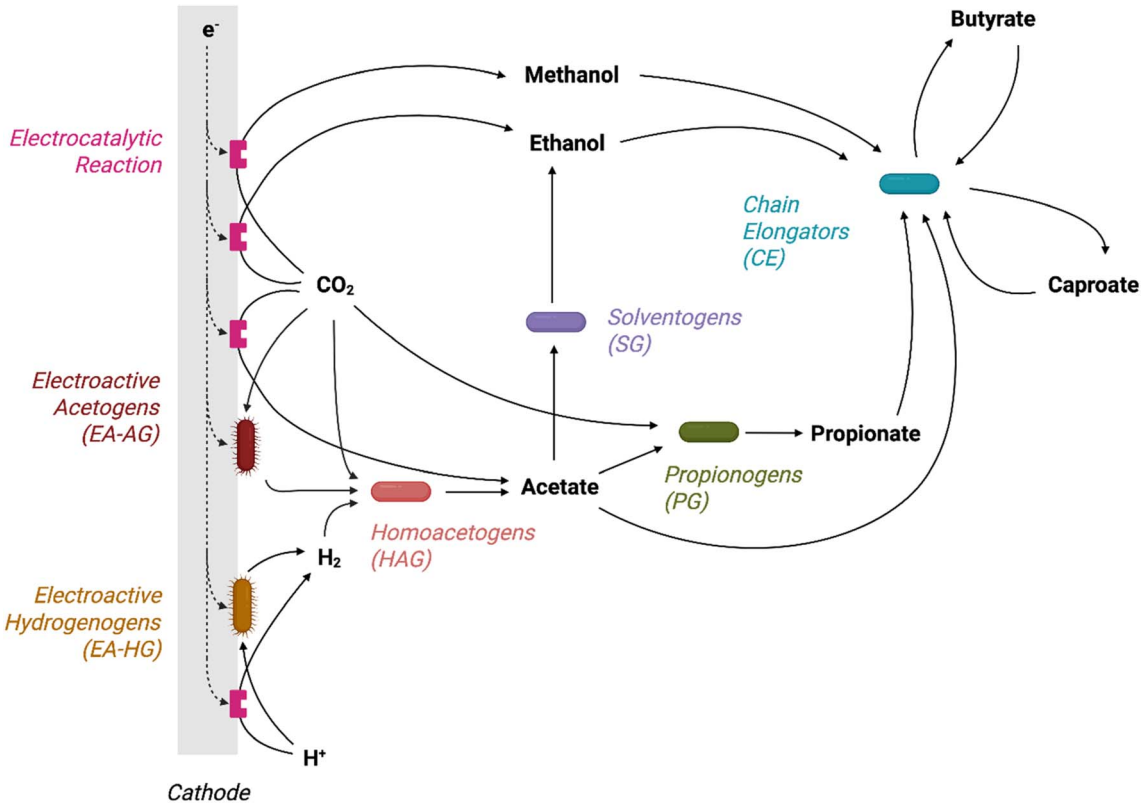

Fig. 7 Simplified conceptual model of microbial caproate production in the MES cells. (Created with BioRender (https://BioRender.com).

for its electroactive hydrogen production,[76] this species likely catalyzed hydrogen generation, complementing the predominantly abiotic electrochemical production expected at the applied voltages.

In the MES1 cell, it is not immediately clear how the initial CO_2 conversion to more reduced organic compounds such as acetate or ethanol proceeded. The microbial communities of MES1 did not include representatives of common homoacetogenic genera such as *Acetobacterium*, *Clostridium*, *Morella*, *Eubacterium*, *Sporomusa*, or *Ruminococcus*.[77] Furthermore, none of the dominant genera in the MES1 cell – bacteria of the genera *Sporanaerobacter*, *Caproiciproducens*, *Megasphaera*, and *Dysgonomonas* – have previously been shown to carry out H_2/CO_2 conversion. The only possible candidate capable of CO_2 conversion in the MES1 cell is a bacterium (ASV26) that was identified belonging to the BRH-c20a clade, and representing 4% of the biofilm community of the MES1 cathode. The BRH-c20a clade has frequently been suggested as being a key player in the electrochemical reduction of CO_2 to acetate.[17,78,79] Interestingly, the closest known relative within the BRH-c20a clade – a bacterium detected in a syngas-based acetate-producing bioreactor (KF956436;[80] – shares only 95% 16S rRNA gene sequence identity with the bacterium detected in the present study, suggesting that ASV18 may represent a new genus or even a new family within this clade. Downstream chain-elongation to butyrate and caproate was likely carried out by populations of *Megasphaera* and, possibly, *Caproiciproducens* detected in the MES1 cell.

In the absence of other possible homoacetogens, the initial CO_2 reduction in the MES2 and MES3 cells was likely also carried out by the detected BRH-c20a bacterium (ASV26) similarly to MES1. However, this bacterium represented only a small fraction (1–2%) of the microbial communities in these cells (Fig. 6). *Clostridium luticellarii*, the dominant homoacetogenic species in the inoculum, was not detected in MES2 and MES3. In the MES2 and MES3 cells, chain elongation to butyrate was likely carried out by populations of *Megasphaera* (ASV1) and the introduced *C. kluyveri* (ASV10).

Overall, the initial conversion of CO_2 through homoacetogenesis appears to have been carried out by bacterial populations present at comparatively low abundance, indicating that this group was the most sensitive to the experimental conditions. Based on this observation, follow-up experiments could be designed to further improve the efficiency and stability of the MES system. The homoacetogens in the original inoculum (*C. luticellarii*) and those eventually detectable in the MES cells (the BRH-c20a bacterium) exhibited very limited growth under the MES operating conditions, as evidenced by their low relative abundance in the microbial communities. In fact, it has been shown that *C. luticellarii* grows very poorly in bioreactors with CO_2 loading rates as were used in this study, thriving best at loading rates nearly an order of magnitude higher.[66] It has also been shown that bacteria associated with BRH-c20a exhibit lower relative abundances in ethanol-fed MES cells (such as the MES2 and MES3 cells in this study) compared to those supplied exclusively with reducing equivalents from an electrode.[17] Given that the low abundance of homoacetogens suggests microbial acetate production could represent a bottleneck in caproate synthesis under the tested MES configuration, enriching or increasing the abundance of the homoacetogenic population may enhance overall caproate yields. Such enrichment could be achieved by increasing the CO_2 loading rate of the MES cells, which might promote the establishment of *C. luticellarii* (from the inoculum) within the system. Alternatively, the homoacetogenic population could be strengthened through bioaugmentation with known electroactive homoacetogens, such as representatives of the genera *Acetobacterium* or *Sporomusa*,[81] which may be better adapted to the conditions of the tested MES setup.

3.6. Electroactivity of cathodic biofilms

To confirm the presence of electroactive bacteria in the catholytes and biofilms of the MES cells, the electrodes were

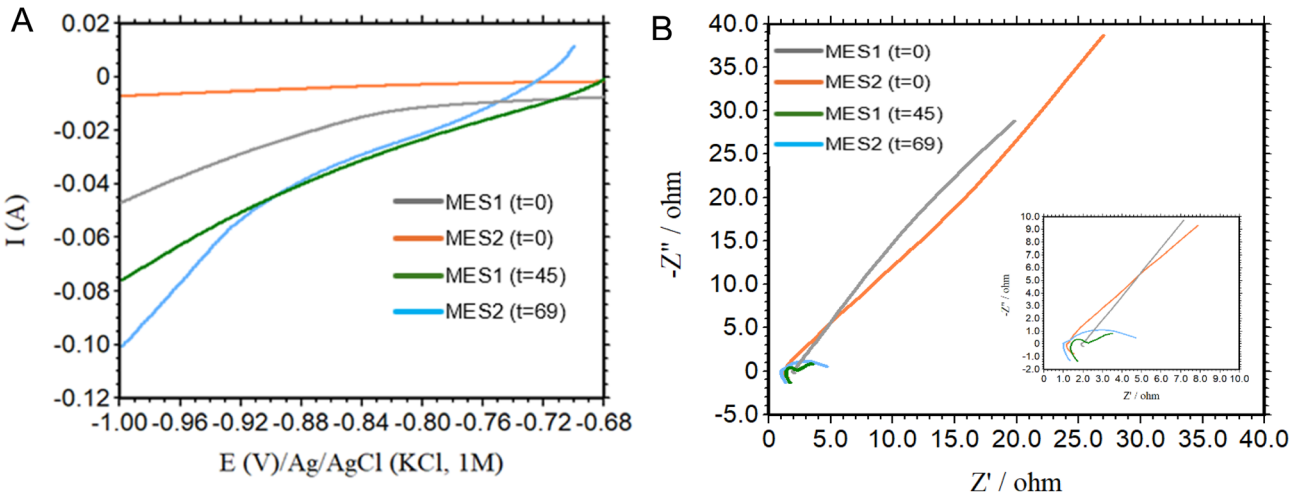

Fig. 8 (A) Linear voltammograms (sweep rate 5 mV s^{-1}) and (B) Nyquist plot recorded during MES1 and MES2 experiments at open circuit voltage.

characterized by cyclic voltammetry and electrochemical impedance spectroscopy (i) immediately after inoculation ($t = 0$), and (ii) at the end of the experiment ($t = 45$ or 69 day) for the MES1 and MES2 cells. The current at the startup of MES1 was more negative than that of MES2 (Fig. 8A). The more negative current observed in MES1 can most likely be attributed to its lower pH (6.0), which promotes the electrochemical hydrogen evolution reaction (HER), relative to MES2 (pH 6.5). For both cells, the observed currents were lower at the end of the experiments than at the beginning, indicating the development of electroactive (*i.e.* electron-consuming) biofilms on the cathodes. This conclusion is consistent with the obtained electrochemical impedance spectroscopy results (Fig. 8B). There, the charge transfer resistance obtained from Nyquist plot fitting decreased from an initial 209 Ω to 0.9 Ω in MES1 and from 302 Ω to 2.3 Ω in MES2 by the end of the experiment. Corresponding microbial community data suggests that the increased cathodic current is a result of the cathode being colonized by the electroactive hydrogen *D. desulfuricans*[76] and electroactive homoacetogens associated with the Bacillota-affiliated BRH-c20a clade.[17]

4. Conclusions

This study demonstrates the effect of bioaugmenting MES cells, inoculated with a mixed acetogenic enrichment, with *Clostridium kluyveri*. Importantly, bioaugmentation with this strain of chain elongating bacteria was combined with the deposition of FeSn bimetallic oxide on the cathode surface resulting in high acetogenic and chain elongating microbial activities. Electrochemical impedance spectroscopy and voltammetry results confirmed the development of electroactive biofilms on cathodes coated with FeSn bimetallic oxide. In the MES1 control cell inoculated solely with the acetogenic enrichment, the main CO_2 reduction products included acetate and butyrate and only small quantities of caproate. In the MES2 and MES3 cells bioaugmented with *C. kluyveri*, caproate production increased more than 8-fold. However, the proliferation and metabolic activity of this chain-elongating bacterium are highly dependent on ethanol supply, implying that further research is needed to overcome this limitation. It can be hypothesized that enhancing ethanol availability – either through the development of a bimetallic oxide cathode for efficient electrochemical ethanol production or through the promotion of microbial ethanol synthesis – can increase the rate of chain elongation. This approach could eliminate the need for an external electron donor and improve selectivity toward caproate production.

Author contributions

T. M.: methodology, investigation, data curation, formal analysis, visualization, writing, review; L. S.: data curation, formal analysis, visualization, writing, review; O. S.: methodology, formal analysis, review; B. T.: conceptualization, methodology, formal analysis, visualization, writing, review, funds acquisition.

Conflicts of interest

The authors declare no competing interests.

Data availability

The data supporting the findings of this study are available within the article. Raw data that support the plots and analyses presented in this work are available from the corresponding author upon request.

Supplementary information (SI) is available. See DOI: https://doi.org/10.1039/d5ra09906d.

Acknowledgements

The research was supported by the National Research Council Canada Materials for Clean Fuels Challenge Program. Assistance of Marie-Josée Levesque (National Research Council of Canada) in sample preparation for 16S rRNA sequencing and carrying out droplet digital PCR (ddPCR) analysis is greatly appreciated. Financial support for T. M. was provided by the Natural Sciences and Engineering Research Council of Canada (NSERC) Discovery Grant program.

References

1 M. A. Shah, A. L. Shibiru, V. Kumar and V. C. Srivastava, Carbon dioxide conversion to value-added products and fuels: opportunities and challenges: a critical review, *Int. J. Green Energy*, 2025, **22**, 1532–1551.
2 Y. Zhang, S. Miao, X. Yuan and J. Zuo, Enhanced conversion of food waste into n-caproate by integrating long-term and short-term fermentation: Performance and mechanisms, *Chem.–Eng. J.*, 2025, 507.
3 S. Agnihotri, D. M. Yin, A. Mahboubi, T. Sapmaz, S. Varjani, W. Qiao, *et al.*, A Glimpse of the World of Volatile Fatty Acids Production and Application: A review, *Bioengineered*, 2022, **13**, 1249–1275.
4 R. Lin, X. Zheng, H. Zhang, Y. He, M. Liu and L. Xie, Cathode catalyst-assisted microbial electrosynthesis of acetate from carbon dioxide: promising material selection, *J. Environ. Sci.*, 2025, **160**(15), 394–404.
5 A. Gomez Vidales, S. Omanovic, H. Li, S. Hrapovic and B. Tartakovsky, Evaluation of biocathode materials for microbial electrosynthesis of methane and acetate, *Bioelectrochemistry*, 2022, 148.
6 N. K. Chaitanya, A. Rajpurohit, P. S. Nair and P. Chatterjee, Enhanced carbon capture and medium chain fatty acid production using microbial electrosynthesis: Role of electrode surface area, *Bioresour. Technol.*, 2025, **435**, 132916.
7 S. Tian, Y. J. Jiang, Y. Cao, J. R. Zhang, Y. Zhou and Y. Wang, Nanomaterials Facilitating Conversion Efficiency Strategies for Microbial CO2 Reduction, *Chem.–Eur. J.*, 2022, **28**, e202202317.
8 I. Ibrahim, M. N. I. Salehmin, K. Balachandran, M. F. Hil Me, K. S. Loh, M. H. Abu Bakar, *et al.*, Role of microbial electrosynthesis system in CO_2 capture and conversion:

a recent advancement toward cathode development, *Front. Microbiol.*, 2023, **14**, 1192187.

9 J. Zhang, H. Liu, Q. Cao, C. Zhang, M. Zhang, M. Cui, *et al.*, Defined Electrosynthetic Microbial Consortia Reveal Electron Transfer Modes Governing Acetate Production, *Adv. Sci.*, 2025, **13**(6), e13340.

10 S. A. Patil, J. B. A. Arends, I. Vanwonterghem, J. Van Meerbergen, K. Guo, G. W. Tyson, *et al.*, Selective Enrichment Establishes a Stable Performing Community for Microbial Electrosynthesis of Acetate from CO2, *Environ. Sci. Technol.*, 2015, **49**(14), 8833–8843.

11 J. S. Deutzmann and A. M. Spormann, Enhanced microbial electrosynthesis by using defined co-cultures, *ISME J.*, 2017, **11**(3), 704–714.

12 J. Du, H. Liang, Y. Zou, B. Li, X. Y. Li and L. Lin, Boosting Microbial CO2 Electroreduction by the Biocompatible and Electroactive Bimetallic Fe-Mn Oxide Cathode for Acetate Production, *ACS Sustain. Chem. Eng.*, 2024, **12**(42), 15659–15670.

13 T. shun Song, T. Li, R. Tao, H. F. Huang and J. Xie, CuO/g-C3N4 heterojunction photocathode enhances the microbial electrosynthesis of acetate through CO2 reduction, *Sci. Total Environ.*, 2022, 818.

14 T. Mihin, O. Savadogo and B. Tartakovsky, Impact of non-noble bimetallic oxides on bioelectrochemical reduction of carbon dioxide to volatile fatty acids, *Process Biochem.*, 2025, **159**, 51–63.

15 K. Tahir, W. Miran, J. Jang, S. H. Woo and D. S. Lee, Enhanced product selectivity in the microbial electrosynthesis of butyrate using a nickel ferrite-coated biocathode, *Environ. Res.*, 2021, 196.

16 N. Chu, W. Hao, Q. Wu, Q. Liang, Y. Jiang, P. Liang, *et al.*, Microbial Electrosynthesis for Producing Medium Chain Fatty Acids, *Engineering*, 2022, **16**, 141–153.

17 Y. Jiang, N. Chu, D. K. Qian and R. Jianxiong Zeng, Microbial electrochemical stimulation of caproate production from ethanol and carbon dioxide, *Bioresour. Technol.*, 2020, 295.

18 M. Wei, X. Zhao, Y. Sun and H. Chen, Recent advances in CO_2 fixation *via* enzymatic catalysis and microbial electrosynthesis systems, *Systems Microbiology and Biomanufacturing*, Springer Nature, 2025.

19 K. Cui, X. Xue, Z. Pan, J. Yu, W. Cai and K. Guo, Selective enrichment of homoacetogens and optimization of the operational conditions for effective acetate production in hydrogen-mediated microbial electrosynthesis reactors, *Biochem. Eng. J.*, 2023, 198.

20 E. Nwanebu, M. Jezernik, C. Lawson, G. Bruant and B. Tartakovsky, Impact of cathodic pH and bioaugmentation on acetate and CH4 production in a microbial electrosynthesis cell, *RSC Adv.*, 2024, **14**(32), 22962–22973.

21 J. Ferretti, R. Minardi, L. Cristiani, M. Villano and M. Zeppilli, Production of Short-chain Fatty Acid from CO2 through Mixed and Pure Culture in a Microbial Electrosynthesis Cell, *Chem. Eng. Trans.*, 2023, **99**, 307–312.

22 C. Zhang, H. Liu, P. Wu, J. Li and J. Zhang, Clostridium kluyveri enhances caproate production by synergistically cooperating with acetogens in mixed microbial community of electro-fermentation system, *Bioresour. Technol.*, 2023, 369.

23 R. Zagrodnik, A. Duber, M. Łężyk and P. Oleskowicz-Popiel, Enrichment *Versus* Bioaugmentation – Microbiological Production of Caproate from Mixed Carbon Sources by Mixed Bacterial Culture and Clostridium kluyveri, *Environ. Sci. Technol.*, 2020, **54**(9), 5864–5873.

24 H. A. Barker and S. M. Taha, Clostridium kluyverii, an organism concerned in the formation of caproic acid from ethyl alcohol, *J. Bacteriol.*, 1942, **43**, 347–363. Available from: https://journals.asm.org/journal/jb.

25 R. K. Thauer, E. Rupprecht and K. Jungermann, The synthesis of one-carbon units from CO2 *via* a new ferredoxin dependent monocarboxylic acid cycle, *FEBS Lett.*, 1970, **8**(5), 304–307, DOI: 10.1016/0014-5793(70)80293-9.

26 M. C. A. A. Van Eerten-Jansen, A. Ter Heijne, T. I. M. Grootscholten, K. J. J. Steinbusch, T. H. J. A. Sleutels, H. V. M. Hamelers, *et al.*, Bioelectrochemical production of caproate and caprylate from acetate by mixed cultures, *ACS Sustain. Chem. Eng.*, 2013, **1**(5), 513–518.

27 C. Koch, A. Kuchenbuch, F. Kracke, P. V. Bernhardt, J. Krömer and F. Harnisch, Predicting and experimental evaluating bio-electrochemical synthesis — A case study with Clostridium kluyveri, *Bioelectrochemistry*, 2017, **118**, 114–122.

28 B. T. Bornstein and H. A. Barker, The Energy Metabolism Of Clostridium kluyveri And The Synthesis Of Fatty Acids, *J. Biol. Chem.*, 1948, **172**, 659–669.

29 R. Gharbi, S. Omanovic, S. Hrapovic, E. Nwanebu and B. Tartakovsky, The Effect of Bismuth and Tin on Methane and Acetate Production in a Microbial Electrosynthesis Cell Fed with Carbon Dioxide, *Molecules*, 2024, **29**(2), 462.

30 A. Escapa, M. F. Manuel, A. Morán, X. Gómez, S. R. Guiot and B. Tartakovsky, Hydrogen production from glycerol in a membraneless microbial electrolysis cell, *Energy Fuels*, 2009, **23**(9), 4612–4618.

31 A. Klindworth, E. Pruesse, T. Schweer, J. Peplies, C. Quast, M. Horn, *et al.*, Evaluation of general 16S ribosomal RNA gene PCR primers for classical and next-generation sequencing-based diversity studies, *Nucleic Acids Res.*, 2013, **41**(1), e1.

32 S. M. McAllister, R. E. Davis, J. M. McBeth, B. M. Tebo, D. Emerson and C. L. Moyer, Biodiversity and emerging biogeography of the neutrophilic iron-oxidizing Zetaproteobacteria, *Appl. Environ. Microbiol.*, 2011, **77**(15), 5445–5457.

33 B. J. Callahan, J. Wong, C. Heiner, S. Oh, C. M. Theriot, A. S. Gulati, *et al.*, High-throughput amplicon sequencing of the full-length 16S rRNA gene with single-nucleotide resolution, *Nucleic Acids Res.*, 2019, **47**(18), E103.

34 Q. Wang, G. M. Garrity, J. M. Tiedje and J. R. Cole, Naïve Bayesian classifier for rapid assignment of rRNA sequences into the new bacterial taxonomy, *Appl. Environ. Microbiol.*, 2007, **73**(16), 5261–5267.

35 M. Chuvochina, J. Gerken, M. Frentrup, Y. Sandikci, R. Goldmann, H. M. Freese, *et al.*, SILVA in 2026: a global core biodata resource for rRNA within the DSMZ digital diversity, *Nucleic Acids Res.*, 2025, **54**(D1), D334–D341, DOI: 10.1093/nar/gkaf1247.

36 H. Wickham, M. Averick, J. Bryan, W. Chang, L. McGowan, R. François, *et al.*, Welcome to the Tidyverse, *J. Open Source Softw.*, 2019, **4**(43), 1686.

37 M. Morgan, S. Anders, M. Lawrence, P. Aboyoun, H. Pagès and R. Gentleman, ShortRead: A bioconductor package for input, quality assessment and exploration of high-throughput sequence data, *Bioinformatics*, 2009, **25**(19), 2607–2608.

38 P. J. McMurdie and S. Holmes, Phyloseq: An R Package for Reproducible Interactive Analysis and Graphics of Microbiome Census Data, *PLoS One*, 2013, **8**(4), e61217.

39 H. Richter, B. Molitor, M. Diender, D. Z. Sousa and L. T. Angenent, A narrow pH range supports butanol, hexanol, and octanol production from syngas in a continuous co-culture of Clostridium ljungdahlii and Clostridium kluyveri with in-line product extraction, *Front. Microbiol.*, 2016, **7**, 1773.

40 N. Krishna Chaitanya, P. S. Nair, A. Rajpurohit and P. Chatterjee, Impact of cell voltage on synthesis of caproic acid from carbon dioxide and ethanol in direct current powered microbial electrosynthesis cell, *Bioresour. Technol.*, 2024, 412.

41 J. Ho Ahn, K. Hwan Jung, E. Seok Lim, S. Min Kim, S. Ok Han and Y. Um, Recent advances in microbial production of medium chain fatty acid from renewable carbon resources: A comprehensive review, *Bioresour. Technol.*, 2023, **381**, 129147.

42 H. Huang, H. Wang, Q. Huang, T. S. Song and J. Xie, Mo2C/N-doped 3D loofah sponge cathode promotes microbial electrosynthesis from carbon dioxide, *Int. J. Hydrogen Energy*, 2021, **46**, 20325–20337.

43 T. Li, K. Zhang, D. Luo, T. S. Song and J. Xie, CuO/g-C3N4/rGO multifunctional photocathode with simultaneous enhancement of electron transfer and substrate mass transfer facilitates microbial electrosynthesis of acetate, *Int. J. Hydrogen Energy*, 2022, **47**(82), 34875–34886.

44 M. Tabish Noori and B. Min, Highly Porous FexMnOy Microsphere as an Efficient Cathode Catalyst for Microbial Electrosynthesis of Volatile Fatty Acids from CO2, *ChemElectroChem*, 2019, **6**(24), 5973–5983.

45 A. H. Anwer, M. D. Khan, N. Khan, A. S. Nizami, M. Rehan and M. Z. Khan, Development of novel MnO2 coated carbon felt cathode for microbial electroreduction of CO2 to biofuels, *J. Environ. Manage.*, 2019, 249.

46 S. Das, S. Das and M. M. Ghangrekar, Application of TiO2 and Rh as cathode catalyst to boost the microbial electrosynthesis of organic compounds through CO2 sequestration, *Process Biochem.*, 2021, **101**, 237–246.

47 G. Wang, Q. Huang, T. S. Song and J. Xie, Enhancing Microbial Electrosynthesis of Acetate and Butyrate from CO2 Reduction Involving Engineered Clostridium ljungdahlii with a Nickel-Phosphide-Modified Electrode, *Energy Fuels*, 2020, **34**(7), 8666–8675.

48 Z. Li, J. Cai, Y. Gao, L. Zhang, Q. Liang, W. Hao, *et al.*, Efficient production of medium chain fatty acids in microbial electrosynthesis with simultaneous bio-utilization of carbon dioxide and ethanol, *Bioresour. Technol.*, 2022, 352.

49 M. V. Reddy, S. V. Mohan and Y. C. Chang, Medium-Chain Fatty Acids (MCFA) Production Through Anaerobic Fermentation Using Clostridium kluyveri: Effect of Ethanol and Acetate, *Appl. Biochem. Biotechnol.*, 2018, **185**(3), 594–605.

50 J. Zhao, H. Ma, W. Wu, M. Ali Bacar, Q. Wang, M. Gao, *et al.*, Conversion of liquor brewing wastewater into medium chain fatty acids by microbial electrosynthesis: Effect of cathode potential and CO2 supply, *Fuel*, 2023, 332.

51 H. Yao, J. M. Rinta-Kanto, I. Vassilev and M. Kokko, Methanol as a co-substrate with CO2 enhances butyrate production in microbial electrosynthesis, *Appl. Microbiol. Biotechnol.*, 2024, **108**(1), 372.

52 P. Batlle-Vilanova, R. Ganigué, S. Ramió-Pujol, L. Bañeras, G. Jiménez, M. Hidalgo, *et al.*, Microbial electrosynthesis of butyrate from carbon dioxide: Production and extraction, *Bioelectrochemistry*, 2017, **117**, 57–64.

53 C. Hiebl, D. Pinner, H. Konegger, F. Steger, D. Mohamed and W. Fuchs, Enhancing Gas Fermentation Efficiency *via* Bioaugmentation with Megasphaera sueciensis and Clostridium carboxidivorans, *Bioengineering*, 2025, **12**(5), 470.

54 Y. J. Lee, C. S. Romanek and J. Wiegel, Clostridium aciditolerans sp. nov., an acid-tolerant spore-forming anaerobic bacterium from constructed wetland sediment, *Int. J. Syst. Evol. Microbiol.*, 2007, **57**(2), 311–315.

55 J. Abrini, H. Naveau and E. J. Nyns, Clostridium autoethanogenum, sp. nov., an anaerobic bacterium that produces ethanol from carbon monoxide, *Arch. Microbiol.*, 1994, **161**(4), 345–351, DOI: 10.1007/BF00303591.

56 R. S. Tanner, L. M. Miller and A. Decheng, Clostridium ljungdahlii sp. nov., an Acetogenic Species in Clostridial rRNA Homology Group I, *Int. J. Syst. Bacteriol.*, 1993, **43**(2), 232–236.

57 F. R. Bengelsdorf, A. Poehlein, S. Linder, C. Erz, T. Hummel, S. Hoffmeister, *et al.*, Industrial acetogenic biocatalysts: A comparative metabolic and genomic analysis, *Front. Microbiol.*, 2016, **7**, 1036.

58 E. Cantos-Parra, S. Ramió-Pujol, J. Colprim, S. Puig and L. Bañeras, Specific detection of "Clostridium autoethanogenum", Clostridium ljungdahlii and Clostridium carboxidivorans in complex bioreactor samples, *FEMS Microbiol. Lett.*, 2018, **365**(18), fny191.

59 T. Makiura, H. C. Tseng, N. Fujimoto and A. Ohnishi, Segatella asaccharophila sp. nov., an anaerobic pectinophile isolated from a two-phase methane fermentation system, *Int. J. Syst. Evol. Microbiol.*, 2024, **74**(12), 006606.

60 C. Petrognani, N. Boon and R. Ganigué, Production of isobutyric acid from methanol by: Clostridium luticellarii, *Green Chem.*, 2020, **22**(23), 8389–8402.
61 B. C. Kim, B. S. Jeon, S. Kim, H. Kim, Y. Um and B. I. Sang, Caproiciproducens galactitolivorans gen. Nov., sp. nov., a bacterium capable of producing caproic acid from galactitol, isolated from a wastewater treatment plant, *Int. J. Syst. Evol. Microbiol.*, 2015, **65**(12), 4902–4908.
62 Y. Kodama, T. Shimoyama and K. Watanabe, Dysgonomonas oryzarvi sp. nov., isolated from a microbial fuel cell, *Int. J. Syst. Evol. Microbiol.*, 2012, **62**(12), 3055–3059.
63 N. Montpart, L. Rago, J. A. Baeza and A. Guisasola, Hydrogen production in single chamber microbial electrolysis cells with different complex substrates, *Water Res.*, 2015, **68**, 601–615.
64 D. M. Hodgson, A. Smith, S. Dahale, J. P. Stratford, J. V. Li, A. Grüning, *et al.*, Segregation of the anodic microbial communities in a microbial fuel cell cascade, *Front. Microbiol.*, 2016, **7**, 699.
65 Y. Dang, D. E. Holmes, Z. Zhao, T. L. Woodard, Y. Zhang, D. Sun, *et al.*, Enhancing anaerobic digestion of complex organic waste with carbon-based conductive materials, *Bioresour. Technol.*, 2016, **220**, 516–522.
66 K. D. Leeuw, M. J. W. van Willigen, T. Vrauwdeunt and D. P. P. T. B. Strik, CO2 supply is a powerful tool to control homoacetogenesis, chain elongation and solventogenesis in ethanol and carboxylate fed reactor microbiomes, *Front. Bioeng. Biotechnol.*, 2024, **12**, 1329288.
67 T. H. Chung, A. Rahman, A. A. Chakrabarty, B. S. Zakaria, M. A. H. Khondoker and B. R. Dhar, 3D printed cathodes for microbial electrolysis cell-assisted anaerobic digester: Evaluation of performance, resilience, and fluid dynamics, *J. Power Sources*, 2024, **15**, 623.
68 J. B. A. Arends, S. A. Patil, H. Roume and K. Rabaey, Continuous long-term electricity-driven bioproduction of carboxylates and isopropanol from CO2 with a mixed microbial community, *J. CO_2 Util.*, 2017, **20**, 141–149.
69 M. J. Medina-Pascual, S. Monzón, P. Villalón, I. Cuesta, F. González-Romo and S. Valdezate, Saezia sanguinis gen. nov., sp. nov., a Betaproteobacteria member of order Burkholderiales, isolated from human blood, *Int. J. Syst. Evol. Microbiol.*, 2020, **70**(3), 2016–2025.
70 S. Q. An, N. Potnis, M. Dow, F. J. Vorhölter, Y. Q. He, A. Becker, *et al.*, Mechanistic insights into host adaptation, virulence and epidemiology of the phytopathogen Xanthomonas, *FEMS Microbiol. Rev.*, 2019, **44**, 1–32.
71 Y. Sun, J. Wei, P. Liang and X. Huang, Electricity generation and microbial community changes in microbial fuel cells packed with different anodic materials, *Bioresour. Technol.*, 2011, **102**(23), 10886–10891.
72 J. Zhang, J. Zhou, Y. Han and X. Zhang, Start-up and bacterial communities of single-stage nitrogen removal using anammox and partial nitritation (SNAP) for treatment of high strength ammonia wastewater, *Bioresour. Technol.*, 2014, **169**, 652–657.
73 L. Chen, M. Wang, Y. Feng, X. Xu, X. Luo and Z. Zhang, Production of bioelectricity may play an important role for the survival of Xanthomonas campestris pv. campestris (Xcc) under anaerobic conditions, *Sci. Total Environ.*, 2021, 768.
74 M. Li, J. C. Bradley, A. R. Badireddy and H. Lu, Ultrafiltration membranes functionalized with lipophilic bismuth dimercaptopropanol nanoparticles: Anti-fouling behavior and mechanisms, *Chem.–Eng. J.*, 2017, **313**, 293–300.
75 M. Romans-Casas, E. Perona-Vico, P. Dessì, L. Bañeras, M. D. Balaguer and S. Puig, Boosting ethanol production rates from carbon dioxide in MES cells under optimal solventogenic conditions, *Sci. Total Environ.*, 2023, 856.
76 E. Perona-Vico, L. Feliu-Paradeda, S. Puig and L. Bañeras, Bacteria coated cathodes as an in-situ hydrogen evolving platform for microbial electrosynthesis, *Sci. Rep.*, 2020, **10**(1), 19852.
77 S. Karekar, R. Stefanini and B. Ahring, Homo-Acetogens: Their Metabolism and Competitive Relationship with Hydrogenotrophic Methanogens, *Microorganisms*, 2022, **10**(2), 397.
78 Y. Gao, Z. Li, J. Cai, L. Zhang, Q. Liang, Y. Jiang, *et al.*, Metal nanoparticles increased the lag period and shaped the microbial community in slurry-electrode microbial electrosynthesis, *Sci. Total Environ.*, 2022, **10**, 838.
79 S. M. Smit, T. D. van Mameren, K. van Zwet, H. P. J. van Veelen, M. Cristina Gagliano, D. P. T. B. Strik, *et al.*, Integration of biocompatible hydrogen evolution catalyst developed from metal-mix solutions with microbial electrosynthesis, *Bioelectrochemistry*, 2024, 158.
80 F. Zhang, J. Ding, N. Shen, Y. Zhang, Z. Ding, K. Dai, *et al.*, In situ hydrogen utilization for high fraction acetate production in mixed culture hollow-fiber membrane biofilm reactor, *Appl. Microbiol. Biotechnol.*, 2013, **97**(23), 10233–10240.
81 J. Philips, Extracellular Electron Uptake by Acetogenic Bacteria: Does H2 Consumption Favor the H2 Evolution Reaction on a Cathode or Metallic Iron?, *Front. Microbiol.*, 2020, 10.